Deep Learning Based Emboli Detection Using Ultrasound Doppler Imaging

Raghava Vinaykanth Mushunuri[*1,2] RAGHAVA.V.MUSHUNURI@NTNU.NO
[1] *Department of Computer Science (IDI), Norwegian University of Science and Technology, Trondheim, Norway*

[2] *Department of Cardiology, St.Olavs, Trondheim, Norway*

Cecilie Le Duc Dahl[*1] CECILIE.DAHL@LYSE.NET
Elisabeth Krogstad Iversen[*1] ELIS.K.IVER@GMAIL.COM
Sigrid Dannheim Vik [3,4] SIGRID.VIK@NTNU.NO
[3] *Department of Circulation and Medical Imaging (ISB), Faculty of Medicine and Health Sciences, NTNU*

Martin Leth-Olsen[3,4] MARTIN.LETH-OLSEN@NTNU.NO
[4] *Children's Clinic, St Olav's University Hospital, Trondheim, Norway*
Magne Gudmundsen[5] MAGNE.GUDMUNDSEN@CIMONMEDICAL.COM
Hans Torp[3,5] HANS.TORP@NTNU.NO
Siri Ann Nyrnes[3,5] SIRI.A.NYRNES@NTNU.NO
[5] *Cimon Medical, Trondheim, Norway*

Gabriel Kiss[1] GABRIEL.KISS@NTNU.NO

Editors: Under Review for MIDL 2026

Abstract

Accurate detection of embolic signals in the bloodstream is crucial for early diagnosis and prevention of cerebrovascular complications, and this work develops and evaluates an artificial intelligence–based system for automatic emboli detection in power Doppler imaging from NeoDoppler, aiming for robust and real-time performance. The study uses a four-stage experimental pipeline built on convolutional neural networks with transfer learning: an initial baseline model (Stage 1), an assessment of spatial generalisation (Stage 2), and a hybrid two-step strategy (Stage 3) that combines conventional High-Intensity Transient Signal (HITS) pre-detection with CNN-based classification, followed by a simplified preprocessing strategy in Stage 4, where single-channel images are replicated into three channels to match pre-trained CNN architectures; all models are trained with 5-fold cross-validation on 523 recordings from 25 patients and evaluated on unseen pilot recordings from the same cohort and additional abdominal surgery data. Across stages, performance improves progressively, with the hybrid two-step framework using the three-channel replication yielding strong results, achieving 96% sensitivity and 98% specificity on the pilot recording and 94% sensitivity and 71% specificity on the abdominal surgery recordings, demonstrating that the proposed approach is an efficient and interpretable solution for ultrasound-based emboli monitoring.

Keywords: Emboli signals, NeoDoppler, High-Intensity Transient Signal, Deep Learning, Transfer Learning

[*] Contributed equally

1. Introduction

Around 1% of all children are born with congenital heart defects. Of these, around 25% will require cardiac surgery or transcatheter intervention. During these interventions, there is a risk of emboli creation, which might enter the bloodstream (O'Brien et al., 1997; Rodriguez et al., 1998; Wallace et al., 2016; LaRovere et al., 2017). Although the clinical implications on children are unclear (Leth-Olsen et al., 2022), neurodevelopmental impairment in children with congenital heart disease is common (Marelli et al., 2016), and cerebral emboli can potentially be harmful. Therefore, neuromonitoring to prevent harmful hemodynamic events during interventions or surgery is important (Andropoulos et al., 2010). Hence, it is paramount to trace the emboli signals entering the bloodstream. Near-infrared spectroscopy has been employed for cerebral monitoring, but it cannot detect microemboli. Transcranial Doppler (TCD) is also used, but it is not helpful in the case of neonates as it requires larger and rigid head for the transducers (Durandy et al., 2011).

Cimon Medical has developed NeoDoppler (see Fig. 1), a new ultrasound device which is lightweight, small and can be gently attached to the fontanel for continuous blood flow monitoring. The Cimon device was clinically tested by Leth-Olsen et al. (2022) and Vik et al. (2020). NeoDoppler's potential in detecting high-intensity transient signals (HITS) containing emboli signals, artefacts, or both was demonstrated by visual inspection of the colour M-mode Doppler recordings. However, time-consuming manual analysis of recordings after intervention procedures is primarily intended for research purposes only (Cullinane et al., 2000). During the actual procedure, it is essential to detect air and solid emboli in real-time. However, this task is highly demanding for clinicians, as it requires them to continuously monitor for emboli while simultaneously performing surgical monitoring. Therefore, implementing automated detection systems becomes critical. These systems can provide real-time alerts to clinicians when emboli signals are detected and would allow for prompt responses and, as such, improve patient outcomes.

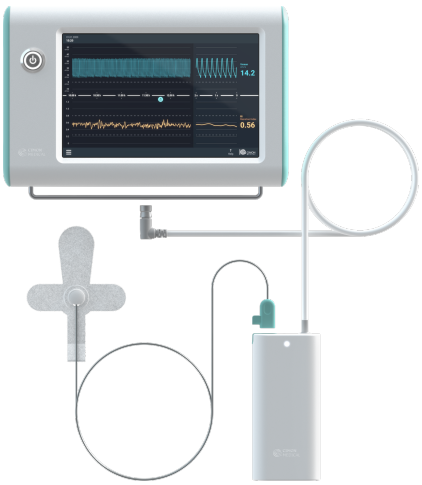

Figure 1: NeoDoppler by Cimon Medical

[1]

1. NeoDoppler device developed by Cimon Medical (https://cimonmedical.com/neodoppler/)

As mentioned above, the formation of emboli comes with its own risks during intervention procedures. Identifying emboli is crucial due to the inherent risks they pose during intervention procedures. Notable research has been done in the lines of conventional signal processing approaches (Cullinane et al., 2000; Geryes et al., 2016; Lam, 2022), but they have a problem in differentiating artefacts from air-emboli.

Cullinane et al. (2000) proposed a single-gate TCD emboli detection approach based on a fixed 3 dB intensity threshold above a median-filtered background signal, while Geryes et al. (2016) similarly applied a constant EBR threshold to spectrogram power for emboli identification. Although computationally simple, these fixed-threshold strategies are highly sensitive to noise and poorly adaptable to patient-specific signal variations, inevitably leading to a high rate of false detections (false positives). More recently, Lam (2022) applied a 15 dB EBR threshold to NeoDoppler power images for neonatal emboli monitoring; however, this method also struggles to reliably distinguish true emboli from artefacts, highlighting the inherent limitations of traditional threshold-based approaches.

Given these challenges, AI plays a crucial role in enhancing the detection of emboli. Convolution Neural Networks (CNNs), since its inception, has been expanding its application, and its footprint is now everywhere, ranging from space applications, underwater robotics, military, drones and many more. Although there is an upsurge in the applications of AI in the medical domain, research related to air-emboli detection is notably sparse (Sombune et al., 2017; Guépié et al., 2018; Grimstad, 2024). Recent advancements in CNNs have significantly improved medical image recognition, diagnosis, and treatment planning.

Sombune et al. (2017) classified embolic signals and artefacts using features from a fixed Doppler frequency range, reporting sensitivities and specificities of 83.0% and 80.1%, respectively. Guépié et al. (2018) explored traditional machine-learning methods such as SVM, Naive Bayes, and Decision Trees on TCD recordings, but performance was limited due to the susceptibility of TCD signals to motion and noise artefacts. More recently, Grimstad (2024) applied deep learning to NeoDoppler data, yet the model demonstrated poor generalisation to unseen pilot recordings, further highlighting the challenge of developing robust emboli detection systems.

In this project, we explored the potential of using AI to detect emboli in real-time within the blood flow during interventions, with a particular focus on detecting larger emboli, which are the ones believed to be of the most clinical significance, while also having a reasonable amount of false detections.

In this experimental study, we systematically examined the impact of three key factors on the performance of state-of-the-art (SOTA) deep learning models for emboli detection: 1) Spatial Position: assessing generalisation to off-center emboli; 2) Hybrid Architecture: evaluating a two-step framework integrating signal processing with deep learning; and 3) Input Processing: investigating the effect of simple three-channel grayscale replication. We trained and identified the best-performing model when compared to others using sensitivity and specificity as evaluation metrics. All the models are trained using 5 fold cross-validation and, were tested subsequently tested on a 30-minute unseen recording from the same cohort. The best performing model was finally tested on 6 recordings from 4 patients who underwent abdominal surgery. Notably, it successfully detected most of the emboli and effectively distinguished artefacts. We also evaluated the model's performance using explainable AI

methods (Saliency maps (Simonyan et al., 2013)) to determine whether the model made decisions based on the significant features of emboli signals.

2. Methods

2.1. Dataset

The dataset for this study includes Power Doppler images containing emboli, normal blood flow, and artefacts or noise signals. These images are extracted from a subset of recordings acquired by Leth-Olsen et al. (2022), who manually annotated all the recordings included in this experiment. Neonates with congenital heart diseases requiring transcatheter interventions or surgery with cardiac pulmonary bypass are continuously monitored using a customised ultrasound probe attached over the anterior fontanelle during the procedure, with prior consent from their parents. However, a few recordings were excluded due to the lack of annotations. All annotations are saved to a CSV file containing timestamps of air-emboli signal locations, the Emboli-to-Blood Ratio (EBR), and the background signal (BGS) intensity. A total of 523 recordings from 25 patients (12 from transcatheter interventions and 13 from surgery) are used in this project. Unseen recording from the same cohort and 6 additional recordings from 4 patients who underwent abdominal surgery (subset of the dataset from Vik et al. (2023) have also been used for further evaluation. All unseen recordings used for evaluation were approximately 30 minutes in duration.

From these recordings, we generated images containing air-emboli signals, which were classified as positive. In contrast, images depicting normal blood flow and artefacts are classified as negative images. Images of 1 second were generated from the timestamps provided in the annotations. These recordings also contain acquisitions at several depth levels. The positive dataset was defined using an Emboli-to-Background Ratio (EBR) threshold of 10.5 dB and a Background Signal (BGS) threshold of $\geq$ 10 dB, while the negative dataset included 80 % artefacts to simulate realistic noise. Images were extracted from power signals at a depth of 12.8 mm (distance from the probe to the tissue).

We performed 5-fold cross-validation, ensuring that the dataset was divided so that there was no overlap between the training, validation, and test sets within each fold. A total of 1,383 images were used for the experiments, with 70% for the training set, 10% for the validation set, and 20% for the test set. All the experiments have $\geq$200 testing samples. Unseen recordings were not included in the training phase and have been used only for evaluating the model's performance. We ensured that there is no class imbalance for all the experiments.

2.2. AI-based emboli detector

Early and reliable detection of embolic signals in ultrasound recordings is crucial for preventing cerebrovascular complications. This section presents the development and evaluation of an artificial intelligence–driven emboli detection system that automates the identification of embolic events in power Doppler imaging. The proposed framework utilises convolutional neural networks (CNNs) with transfer learning to distinguish between embolic and non-embolic signals under various imaging and noise conditions.
The study is structured into four successive stages. In Experiment 1, baseline CNN mod-

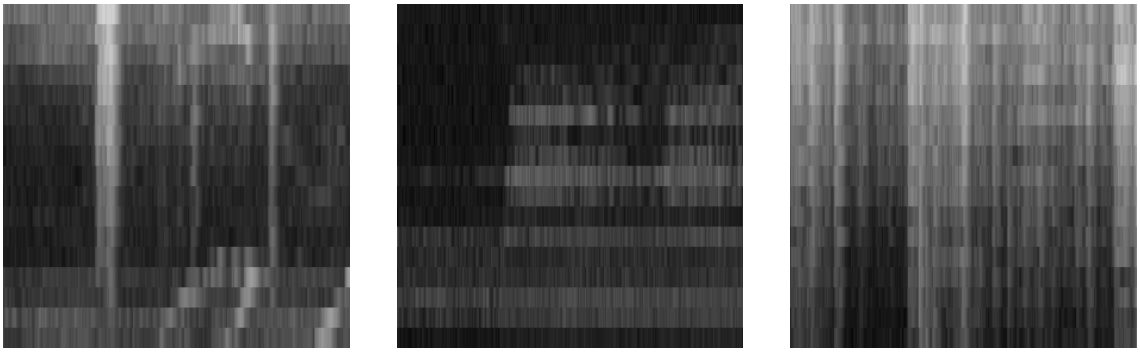

(*a*) Air-emboli + noise (*b*) Normal blood flow (*c*) Artifact

Figure 2: Example images for experiments: (a) shows both artefacts and embolic signals, (b) shows a blood flow signal, and (c) shows an artefact signal.

els are retrained using images where embolic events are temporally centred, establishing the core detection performance. Experiment 2 assesses model generalisation by introducing emboli that appear at spatial or temporal offsets within the imaging frame. Building upon these results, Experiment 3 introduces a hybrid two-step detection framework that combines signal processing for initial event localisation with CNN-based classification to increase accuracy and reduce false positives. Finally, Experiment 4 investigates a simplified preprocessing approach in which the single-channel ultrasound images are directly replicated across three channels, enabling straightforward compatibility with pretrained CNN architectures.

Each stage incrementally improves model robustness, accuracy, and suitability for real-time clinical deployment in ultrasound-based emboli monitoring.

2.2.1. **Centered Emboli:**

The first experiment evaluated the performance of various CNN architectures—VGG16 (Simonyan and Zisserman, 2014), ResNet101(He et al., 2016), EfficientNet-V2(Tan and Le, 2021), MobileNet-V3(Howard et al., 2019)—for detecting centred embolic signals in ultrasound power Doppler images.

Here, centred emboli refer to image segments extracted such that the embolic event is temporally centred within the sample window. Based on the manually annotated timestamps from the original ultrasound recordings, each embolic signal was extracted with a 0.5-second margin on either side of the event. This ensured that the embolus appeared approximately in the middle of each image and that contextual signal information before and after the embolus was preserved.

To adapt single-channel that expect RGB input, an additional convolutional layer was introduced to map the grayscale input tooduced to map the grayscale input into three channels. The pretrained feature extractor layers were kept frozen, and only the first and final classification layers were retrained. The classification head was replaced with a single-neuron output (without activation) for binary prediction. This experiment replicates Grimstad et al.'s(Grimstad, 2024) recent contributions to emboli detection using deep learning.

2.2.2. Emboli with offset:

The second experiment extended the baseline model to assess detection robustness when embolic events occurred at varying spatial or temporal offsets relative to the image centre. Using the same architectures and training protocols as in Stage 1, the networks were retrained on a dataset containing off-centre emboli while maintaining the same negative samples. This experiment evaluated spatial generalisation—specifically, the model's ability to maintain detection accuracy when emboli appear at different positions within the field of view.

2.2.3. **Two step approach:**

After training models with and without emboli offset, we employed a two-step approach as portrayed in 3. The two-step detection framework consists of an initial signal-processing stage followed by deep-learning classification. In the first step, high-intensity transient signals (HITS) are extracted from the raw Doppler recordings using the threshold-based method described by (Lam, 2022), generating candidate regions that may contain both embolic signals and noise. In the second step, the two best-performing CNN architectures from the earlier experiments are fine-tuned to classify each candidate region as embolic or non-embolic, using the same dataset configuration, cross-validation strategy, and training setup as in the previous stages.

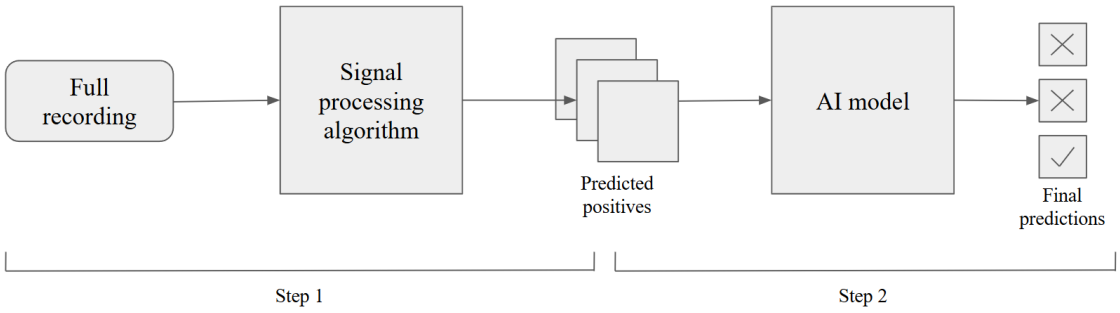

Figure 3: Visualization of the two-step method.

2.2.4. Three channel replication:

The final experiment explored an alternative and computationally simpler preprocessing approach. Instead of applying a learnable convolutional layer to expand grayscale ultrasound images, the single channel was directly replicated across three channels to satisfy the input requirements of pretrained CNNs. This method preserved the intrinsic intensity distribution of the ultrasound data while simplifying the preprocessing pipeline.

Models were trained and validated on datasets encompassing emboli with a wide range of EBR values to assess the effect of signal intensity variation on classification performance.

2.3. End-To-End pipeline testing

The best performing model, when evaluated on the pilot recording, is used for further evaluation using 6 additional unseen recordings. As described in the 2.1, these recordings are obtained from patients who underwent abdominal surgery. It contained a total of 13,500 images, out of which only 26 were images that contained embolic signals. The remaining ones are either blood flow images or artefact images. Images are acquired with an offset and 25% overlap. The evaluation metrics are same as mentioned in 2.4.

In addition to the use of the model in an emboli alarm system, we wanted to create a tool that could support emboli research by assisting with the annotation of ultrasound recordings. We developed a processing pipeline for ultrasound recordings that first applies Lam's algorithm, then passes the resulting data through our CNN model, and finally outputs the automatic detections generated by the system. To enable local deployment of the model, we used onnx. The trained model – loaded with the best-performing weights and set to evaluation mode – was exported to a .onnx file. This exported model was then used for evaluation in the same way as usual.

2.4. Evaluation

Evaluation is paramount to estimate the performance of the models and it is crucial in medical imaging domain, where misclassification can lead to risky repercussions. It is also crucial identify potential bias if present. There are two types of evaluation procedures namely, quantitative evaluation and qualitative evaluation. Quantitative evaluation is done using standard metrics, such as accuracy, sensitivity, specificity and F1 score. These metrics are calculated using confusion matrix. Explainable AI (XAI) involves methods and techniques, which helps humans perceive the decision making process of an AI model by providing insights on how it arrived at a particular decision/s (Samek et al., 2017; Gilpin et al., 2018). Saliency maps visualisation is a technique, that highlight the regions of an input image that most strongly influence a model's prediction, offering a visual explanation of where the network focuses. (Simonyan et al., 2013). In this project, we used this method to understand model's behaviour when testing it on unseen recording.

2.5. Training details

Networks are trained using PyTorch framework on NVIDIA RTX A6000, and Torchvision library is used for pre-trained model weights and they corresponds to Imagenet dataset, For XAI techniques, we have used Captum library. Image dimensions are originally 289 $\times$ 291 $\times$ 1 and then reshaped to 256 $\times$ 256 $\times$ 1 using a nearest neighbour interpolation technique. Later a convolution layer is added to obtain a three-channel (see 2.2.1) image of size 224 $\times$ 224 $\times$ 3, which is standard image dimension expected by the models. Images are loaded using PIL (pillow) library and the images are divided by maximum value to have a pixel range of 0-1.0. Batch size is set to 32 and learning rate of 1×10^{-2} is used. Binary cross-entropy loss is used as the loss function, and the ADAM optimiser is used for optimising model weights. Models are initially trained for 400 epochs but later we changed to 200 as models are converging around 200All the models are trained for 5-fold cross-validation, and the dataset is divided accordingly.ordingly.

3. Results and Evaluation

All the experiments are evaluated quantitatively using standard evaluation metrics specified in 2.4 and qualitative analysis is done on unseen recordings using XAI methods as specified in 2.4. The results of each experiment are described below and are also summarised in 1, 2.

Experiment 1								
Model	**Accuracy**	**Precision**	**Sensitivity**	**Specificity**	**TP**	**FP**	**FN**	**TN**
VGG16	65%	3%	72%	64%	26	840	10	1522
EfficientNet	95%	11%	33%	96%	12	94	24	2268
ResNet101	96%	19%	50%	96%	18	75	18	2287
MobileNet	95%	7%	19%	96%	7	93	29	2269
DenseNet	82%	4%	50%	83%	18	404	18	1958
Experiment 2								
Model	**Accuracy**	**Precision**	**Sensitivity**	**Specificity**	**TP**	**FP**	**FN**	**TN**
VGG16	11%	2%	94%	10%	34	2131	2	231
EfficientNet	81%	1%	17%	82%	6	433	30	1929
ResNet101	19%	2%	83%	18%	30	1934	6	428
MobileNet	52%	2%	58%	52%	21	1141	15	1221
DenseNet	17%	2%	92 %	16%	33	1984	3	378
Experiment 3								
Model	**Accuracy**	**Precision**	**Sensitivity**	**Specificity**	**TP**	**FP**	**FN**	**TN**
VGG16	96%	51%	96%	96%	25	24	1	561
ResNet101	94%	40%	88%	94%	23	35	3	550

Table 1: Evaluation metrics of experiments 1, 2 and 3.

3.1. Experiment-1: Images with centered emboli signals

All the SOTA models were evaluated using 5-fold cross-validation, and the best performing model from the 5 folds was evaluated using Pilot recording, which is not part of the training and validation phase. All the models were evaluated using evaluation metrics as described in 2.4. VGG16 and ResNet101 models performed well during the validation phase; however, when tested on pilot recordings, the models failed to identify various signals, due to the fact that the emboli signals are not centred.

We further evaluated the performance of the approach from experiment-4 qualitatively using the saliency maps method with pilot-recording, and the heatmaps are shown in Figure. 4.

3.2. Experiment-2: Emboli signals with offset

To observe the change in model performance, we trained all models from Experiment 1 using offset emboli signals as described in section-2.2.2. The models performed with nearly perfect accuracy during the validation phase. Although the evaluation showed improved performance from the previous experiment stage, they still failed to reduce the false positives on the pilot recording.

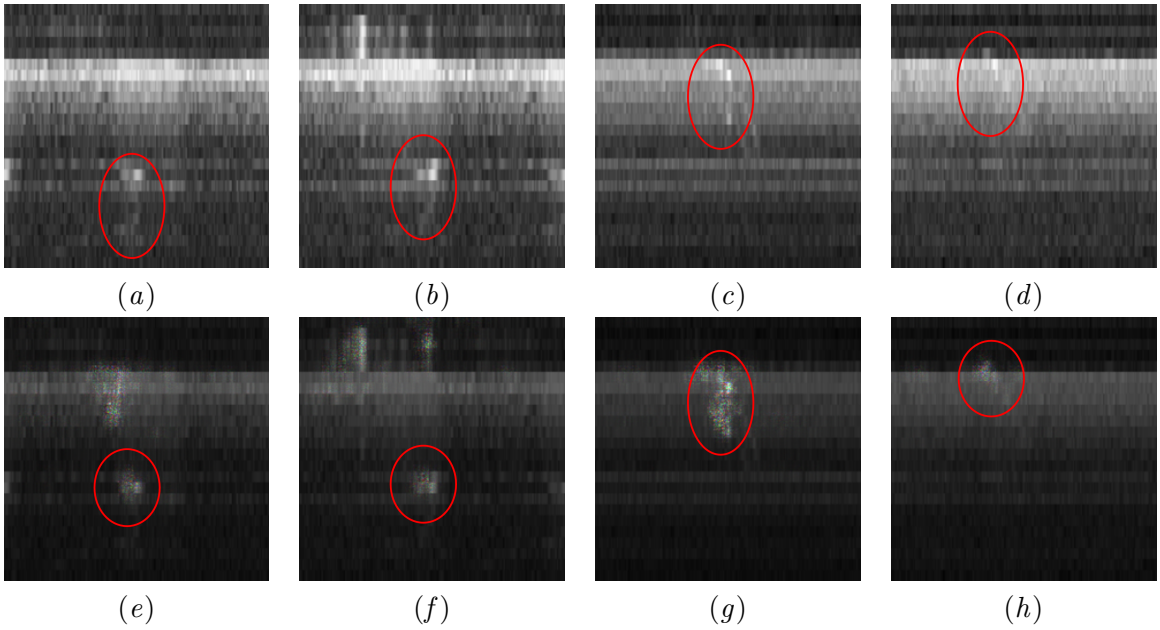

Figure 4: XAI heatmaps for true positive predictions with unseen recording: subfigures (a), (b), (c), and (d) are the original images, while (e), (f), (g), and (h) are the corresponding heatmaps overlaid on the original images. Emboli regions and the saliency maps are highlighted in both original and overlayed maps.

Model	parameter	Accuracy	Precision	Sensitivity	Specificity	TP	FP	FN	TN
Experiment 4									
VGG16	ebr 10.5	98%	68%	96%	98%	25	12	1	573
VGG16	ebr 7	95%	45%	96%	95%	25	31	1	554
VGG16	ebr 4	98%	75%	92%	99%	24	8	2	577
Experiment 4									
ResNet101	ebr 10.5	98%	68%	96%	98%	25	12	1	573
ResNet101	ebr 7	97%	60%	96%	97%	25	17	1	568
ResNet101	ebr 4	97%	57%	92%	97%	24	18	2	567

Table 2: Evaluation metrics of VGG16 and ResNet101 after swapping to three-channel replication (experiment-4).

3.3. Experiment-3: Two-step approach

To further reduce the false positives, we used two steps. In the first step, we filtered the pure blood flow signals from HITS, and in the second step, we classified the HITS as emboli or artefact signals using deep learning algorithms. For this, we have chosen the VGG16 and ResNet101 models for training, as they both performed well in the previous experiment stages.

3.4. Experiment-4: Three channel replication

Although the two-step approach performed well, there is still room for improvement. We experimented further by replicating the gray scale array to form 3 channels, and we observed that there is a significant rise in the specificity. We focused solely on improving specificity, which implies we focused on reducing false positives. As shown in Table. 2, we can see that the unseen recording testing shows the false positive prediction is reduced by a greater extent.

3.5. Evaluation of end-end pipeline

The best-performing model is evaluated using unseen recordings from abdominal surgery, which were not part of the training and validation cycle, and are evaluated using the same metrics. The two-step approach with 3-channel replication performed well during the cross-validation phase, hence we evaluated that approach further.

	Accuracy	**Precision**	**Sensitivity**	**Specificity**	**TP**	**FP**	**FN**	**TN**	**Total negative**
Without intervention	82%	73%	94%	71%	16	6	1	15	13540
Intervention	85%	81%	96%	71%	25	6	1	15	13549

Table 3: Evaluation metrics of ResNet101 on new test data.

	False alarms	**False alarms/minute**
Baseline	88	2.9
Our work	7	0.23

Table 4: A comparison of the false alarm rate between Grimstad's model and our model.

When tested on the pilot recording from the same cohort, the two-step approach only missed one emboli signal as shown in Table. 2. When this approach is tested on recordings from abdominal surgery, we missed 7 emboli signals in the first stage. We manually added the missed emboli signals to check if the model without a filtering algorithm can detect the missed emboli signals. The model detected all 7 missed signals. Evaluation metrics on unseen recordings are shown in Table. 3. We later designed an alarm system to estimate the false-positive rate per minute during this evaluation phase and observed that our approach produced only 7% of the total false alarms compared (see Table. 4) to the baseline model from experiment-1 by (Grimstad, 2024).

4. Discussion

The aim of this work is to detect emboli entering cerebral circulation in real-time using deep learning. We conducted an experimental study by training state-of-the-art (SOTA) models at various stages and observing how their performance changed with different dataset

modifications. Across all experiments, the results consistently highlight both the promise and the challenges of applying CNNs to emboli detection. Experiment 1, which replicates (Grimstad, 2024), demonstrated that deep learning models can be utilised to detect emboli signals. When the models are tested using 5-fold cross-validation, the metrics were observed to be near perfect values, however, when tested on pilot unseen recording, the models raised a massive number of false alarms and we also observed that the main drawback of this experiment is that it is biased towards the position of emboli signals, as the models were trained on centred emboli signals. To overcome the drawbacks of this experiment, we trained the models with offset emboli and achieved better performance compared to the models trained in Experiment 1. Experiment 2 demonstrated that positional robustness can be achieved, ensuring models rely on embolic features rather than fixed spatial features. We observed that sensitivity and specificity improved gradually when tested on a pilot recording. However, all the models still generated a high amount of false positives. For further experiments, we selected VGG16 and ResNet101 models, as there is no substantial improvement in the performance of other models. Experiment 3 further improved performance by integrating a two-step approach, in which classical signal processing substantially reduced false positives without compromising sensitivity, underscoring the need for additional improvements to achieve a robust model. Pertaining to the above reasons, we introduced a two-stage classifier model, as explained in Section 3 of the methods. This method reduced false positives further and improved sensitivity in a pilot recording, but the false-positive rate remains considerable. Experiment 4 demonstrated that simple three-channel replication is both more stable and effective than convolutional projection, significantly reducing false positives and proving to be a practical input strategy. ResNet101 model performed well during the evaluation phase. XAI evaluation using saliency maps on the unseen recording also showed that the model is looking at the patterns in the emboli signals and making predictions, indicating that the models are not predicting garbage and that the projections are based on meaningful features (see Figure. 4).

While evaluating the end-to-end pipeline using a two-step approach on 6 unseen recordings with a signal, we designed an alarm system to track false-alarm frequency per minute and found it was as low as 0.23 per minute. We also designed a MATLAB-based GUI to load the recording and detect the emboli signals. For this, the models are converted to ONNX, allowing them to run on CPUs as well, rather than just GPU-based inference. The testing was done seamlessly without any reduction in performance.

Although the two-step approach performed well during initial evaluation, when tested on unseen recordings from abdominal surgery, it missed a few emboli signals. This could be due to the reason that the emboli signals from those recordings have EBR $\leq$ 4 db and Lam's algorithm works better for higher EBR values.

5. Conclusion

In conclusion, we developed a two-step approach to detect emboli signals in the bloodstream. The first step is a simple signal processing algorithm which detects HITS, and the second step identifies whether the filtered signal is an emboli or an artefact. We also integrated an ONNX model for inference using a CPU with a simple GUI.

Acknowledgments

The authors would like to acknowledge the contributions of Arild Grimstad who implemented the initial experiments during his master thesis. Raghava Vinaykanth Mushunuri has received funding from the Liaison Committee for Education, Research and Innovation in Central Norway (project number:2023-34188).

References

Dean B Andropoulos, Jill V Hunter, David P Nelson, Stephen A Stayer, Ann R Stark, E Dean McKenzie, Jeffrey S Heinle, Daniel E Graves, and Charles D Fraser Jr. Brain immaturity is associated with brain injury before and after neonatal cardiac surgery with high-flow bypass and cerebral oxygenation monitoring. *The Journal of thoracic and cardiovascular surgery*, 139(3):543–556, 2010.

Marisa Cullinane, Greg Reid, Ralf Dittrich, Zoltan Kaposzta, Rob Ackerstaff, Viken Babikian, Dirk W Droste, Donald Grossett, Mario Siebler, Luc Valton, et al. Evaluation of new online automated embolic signal detection algorithm, including comparison with panel of international experts. *Stroke*, 31(6):1335–1341, 2000.

Y Durandy, M Rubatti, and R Couturier. Near infrared spectroscopy during pediatric cardiac surgery: errors and pitfalls. *Perfusion*, 26(5):441–446, 2011.

Maroun Geryes, Sebastien Ménigot, Walid Hassan, Ali Mcheick, Jamal Charara, and Jean-Marc Girault. Detection of doppler microembolic signals using high order statistics. *Computational and mathematical methods in medicine*, 2016(1):3243290, 2016.

Leilani H Gilpin, David Bau, Ben Z Yuan, Ayesha Bajwa, Michael Specter, and Lalana Kagal. Explaining explanations: An overview of interpretability of machine learning. In *2018 IEEE 5th International Conference on data science and advanced analytics (DSAA)*, pages 80–89. IEEE, 2018.

Bror Arild Grimstad. Automatic detection of embolic signals in doppler m-mode images using deep learning. Master's thesis, NTNU, 2024.

Blaise Kevin Guépié, Matthieu Martin, Victor Lacrosaz, Marilys Almar, Benoit Guibert, and Philippe Delachartre. Sequential emboli detection from ultrasound outpatient data. *IEEE Journal of Biomedical and Health Informatics*, 23(1):334–341, 2018.

Kaiming He, Xiangyu Zhang, Shaoqing Ren, and Jian Sun. Deep residual learning for image recognition. In *Proceedings of the IEEE conference on computer vision and pattern recognition*, pages 770–778, 2016.

Andrew Howard, Mark Sandler, Grace Chu, Liang-Chieh Chen, Bo Chen, Mingxing Tan, Weijun Wang, Yukun Zhu, Ruoming Pang, Vijay Vasudevan, et al. Searching for mobilenetv3. In *Proceedings of the IEEE/CVF international conference on computer vision*, pages 1314–1324, 2019.

My Tam Lam. Automatic detection of air emboli in the cerebral circulation in newborns by ultrasound doppler technique. Master's thesis, NTNU, 2022.

Kerri L LaRovere, Kush Kapur, Doff B McElhinney, Alexander Razumovsky, and Barry D Kussman. Cerebral high-intensity transient signals during pediatric cardiac catheterization: A pilot study using transcranial doppler ultrasonography. *Journal of Neuroimaging*, 27(4):381–387, 2017.

Martin Leth-Olsen, Gaute Døhlen, Hans Torp, and Siri Ann Nyrnes. Detection of cerebral high-intensity transient signals by neodoppler during cardiac catheterization and cardiac surgery in infants. *Ultrasound in Medicine & Biology*, 48(7):1256–1267, 2022.

Ariane Marelli, Steven P Miller, Bradley Scott Marino, Angela L Jefferson, and Jane W Newburger. Brain in congenital heart disease across the lifespan: the cumulative burden of injury. *Circulation*, 133(20):1951–1962, 2016.

James J O'Brien, John Butterworth, John W Hammon, Kristin J Morris, Julia M Phipps, and David A Stump. Cerebral emboli during cardiac surgery in children. *The Journal of the American Society of Anesthesiologists*, 87(5):1063–1069, 1997.

Rosendo A Rodriguez, Martin C Hosking, Walter J Duncan, Brian Sinclair, Otto HP Teixeira, and Garry Cornel. Cerebral blood flow velocities monitored by transcranial doppler during cardiac catheterizations in children. *Catheterization and cardiovascular diagnosis*, 43(3):282–290, 1998.

Wojciech Samek, Thomas Wiegand, and Klaus-Robert Müller. Explainable artificial intelligence: Understanding, visualizing and interpreting deep learning models. *arXiv preprint arXiv:1708.08296*, 2017.

Karen Simonyan and Andrew Zisserman. Very deep convolutional networks for large-scale image recognition. *arXiv preprint arXiv:1409.1556*, 2014.

Karen Simonyan, Andrea Vedaldi, and Andrew Zisserman. Deep inside convolutional networks: Visualising image classification models and saliency maps. *arXiv preprint arXiv:1312.6034*, 2013.

Praotasna Sombune, Phongphan Phienphanich, Sutanya Phuechpanpaisal, Sombat Muengtaweepongsa, Anuchit Ruamthanthong, and Charturong Tantibundhit. Automated embolic signal detection using deep convolutional neural network. In *2017 39th Annual International Conference of the IEEE Engineering in Medicine and Biology Society (EMBC)*, pages 3365–3368. IEEE, 2017.

Mingxing Tan and Quoc Le. Efficientnetv2: Smaller models and faster training. In *International conference on machine learning*, pages 10096–10106. PMLR, 2021.

Sigrid D Vik, Hans Torp, Anders H Jarmund, Gabriel Kiss, Turid Follestad, Ragnhild Støen, and Siri Ann Nyrnes. Continuous monitoring of cerebral blood flow during general anaesthesia in infants. *BJA open*, 6:100144, 2023.

Sigrid Dannheim Vik, Hans Torp, Turid Follestad, Ragnhild Støen, and Siri Ann Nyrnes. Neodoppler: new ultrasound technology for continuous cerebral circulation monitoring in neonates. *Pediatric research*, 87(1):95–103, 2020.

Sean Wallace, Gaute Døhlen, Henrik Holmstrøm, Christian Lund, and David Russell. Cerebral microemboli detection and differentiation during transcatheter closure of patent ductus arteriosus. *Pediatric cardiology*, 37:1141–1147, 2016.